

Unconventional roles of metal catalysts in chemical-vapor syntheses of single-crystalline nanowires

Kibum Kang,¹ Cheol-Joo Kim,¹ and Moon-Ho Jo^{1,2,a)}

¹Department of Materials Science and Engineering, Pohang University of Science and Technology (POSTECH), San 31, Hyoja-Dong, Nam-Gu, Pohang, Gyungbuk 790-784, Republic of Korea

²Graduate Institute of Advanced Materials Science, Pohang University of Science and Technology (POSTECH), San 31, Hyoja-Dong, Nam-Gu, Pohang, Gyungbuk 790-784, Republic of Korea

(Received 24 August 2008; accepted 17 March 2009; published online 18 June 2009)

In this invited contribution at the 29th International Conference on the Physics of semiconductors (ICPS 2008), we review two examples of solid-catalytic nanowire (NW) growth in parallel comparisons to the NW growth from the eutectic liquid catalyst. First, we demonstrated the Cu-catalyzed Ge NW growth using GeH₄ vapor precursor at 200 °C, which is far below the Cu–Ge eutectic temperature of 644 °C, with a relatively uniform diameter distribution directly templated from that of the catalysts. We provide evidence that the formation of solid Cu₃Ge catalysts and Ge diffusion across the catalysts are responsible for such low-temperature growth of Ge NWs in a size-deterministic manner. Second, we show the spontaneous silicidation of NiSi_x NWs on continuous Ni bulks using SiH₄ vapor precursor at 400 °C. This growth is particularly marked in that NiSi_x NWs are formed in a self-organized manner without employing the nanocluster catalysts. We discuss this spontaneous growth of NiSi_x NWs within the frame of the nucleation kinetics in the low supersaturation limit in analogous with the earlier examples of the vapor-condensation at the low vapor pressures. © 2009 American Institute of Physics. [DOI: 10.1063/1.3117233]

I. INTRODUCTION

Single-crystalline nanowire (NW) growth in the vapor phases typically requires metal catalysts of nanometer sizes for the catalytic decomposition of the vapor precursors, the dimensionally confined nucleation, and the subsequent one-dimensional growth. One of the prominent examples for the growth of semiconductor NWs is the metal-catalytic chemical-vapor growth of Si and Ge NWs,^{1–3} where these metal nanoclusters conventionally serve for the catalytic crystallization as eutectic liquids. Thereby the thermodynamic limit of such metal-catalytic NW growth is largely set by the lowest eutectic temperature of the binary systems of metals and semiconductors; for example the (Au, Si) and (Au, Ge) binary systems find them to be around 360–370 °C in the bulk limit. Recently it has been reported that the specific phase of the catalysts is not necessarily the simple eutectic liquids during the growth reactions, but can be also the solid phases.^{4–10} In this invited contribution, we describe two representative examples of such *unconventional* NW synthetic routes, where Cu and Ni catalysts involve in the NW growth reactions as the solid-phases. Specifically we illustrate Ge NW growth from Cu nanoparticles¹⁰ and the NiSi_x NW growth from continuous Ni bulks,^{11,12} in direct comparisons to the growth from the eutectic liquid catalyst of Au. First, we demonstrate the Cu-catalyzed Ge NW growth using GeH₄ chemical vapors at 200 °C in the (Cu, Ge) binary system, whose eutectic temperature is at 644 °C. It was found that the formation of Cu₃Ge catalysts in solid-phase and Ge diffusion across the catalysts are responsible for such low-temperature growth of Ge NWs in a size-deterministic

manner between catalysts and NWs. Second, from the (Si, Ni) binary system, whose eutectic temperature is above 960 °C, we show the spontaneous growth of NiSi_x NWs on continuous Ni bulks using SiH₄ chemical vapors at 400 °C by silicidations. We discuss this spontaneous one-dimensional silicidation without employing the nanocluster catalysts within the framework of the nucleation kinetics and the subsequent one-dimensional diffusion. Therein we attempt to draw analogy with the earlier examples of the vapor-condensation into metal whiskers in the low supersaturation limit.

II. CU-CATALYZED GE NW GROWTH

Figure 1 shows the schematics and the sequential snapshots in the early growth stages of two different types of Ge NWs grown by Au and Cu catalysts at 330 and 275 °C in parallel comparison. Nanoclusters of Au and Cu catalysts were prepared by deposition of discontinuous films of the nominal thickness of 0.5 nm on SiO₂/Si (100) and were subsequently loaded into a hot-walled quartz-tube furnace, where we carry out chemical vapor deposition (CVD) of GeH₄. Figure 1(b) is the equilibrium Ge–Cu binary phase diagram,¹³ where the marked region is relevant to our growth conditions. Notably the Ge–Cu eutectic temperature of 644 °C is too high to grow Ge NWs by the eutectic liquid because above 300 °C the thermal decomposition of GeH₄ becomes homogeneously active over the catalytic decomposition.^{14,15} Whereas the Au-catalyzed Ge NW growth can be available by the presence of the Au–Ge eutectic liquid at the growth conditions, as in Fig. 1(g). High resolution transmission electron microscope (TEM) study on Cu-catalyzed Ge NWs demonstrate that both the catalytic tip

^{a)}Electronic mail: mhjo@postech.ac.kr.

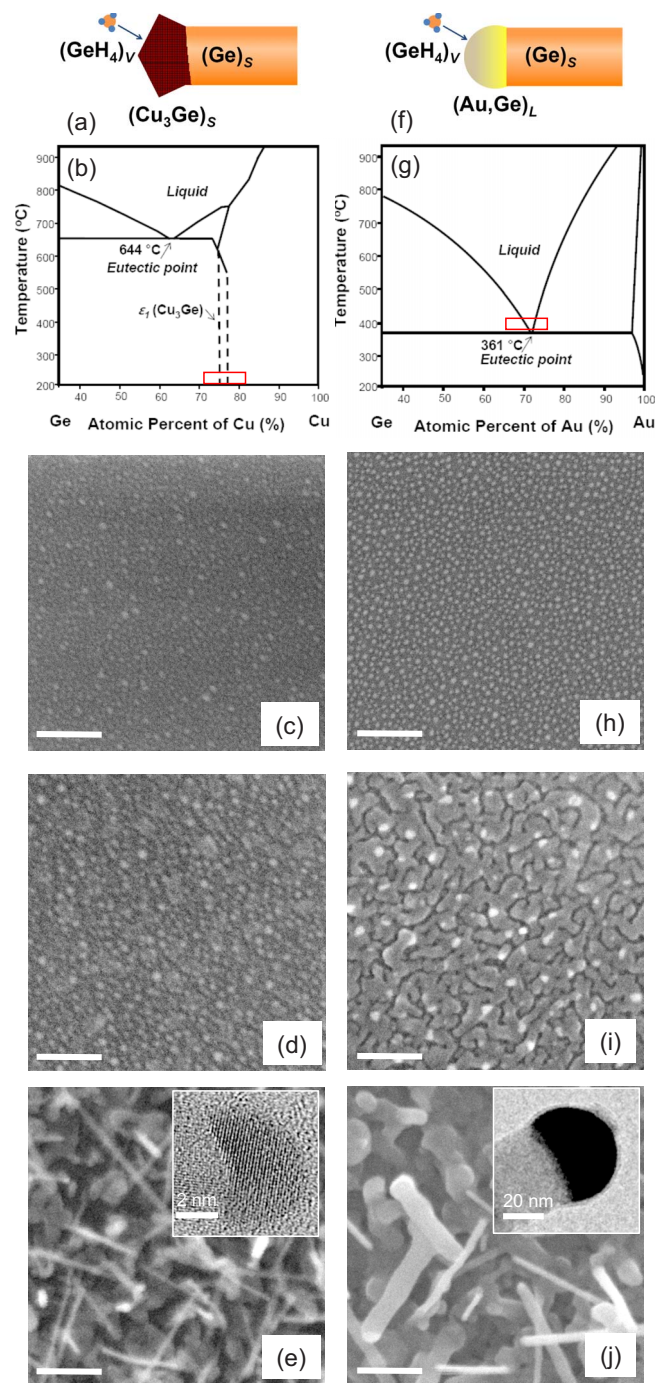


FIG. 1. (Color online) (a) The schematics of Cu catalytic growth of Ge NWs. (b) A part of the equilibrium Cu–Ge binary alloy phase diagram, where the marked region is relevant to our growth conditions. (c) Thermally evaporated 0.5 nm thick Cu films before the GeH_4 CVD. (d) The initial stage of the GeH_4 CVD for 5 s on 0.5 nm thick Cu films. (e) The 2 min of the GeH_4 CVD on 0.5 nm thick Cu films. The inset shows TEM image of an individual Ge NW grown by Cu catalyst at the tip region. (f) The schematics Au catalytic growth of Ge NWs. (g) A part of the equilibrium Au–Ge binary alloy phase diagram, where the marked region is relevant to our growth conditions. (h) Thermally evaporated 0.5 nm thick Au films before the GeH_4 CVD. (i) The initial stage of the GeH_4 CVD for 5 s on 0.5 nm thick Au films. (j) The 30 s GeH_4 CVD on 0.5 nm thick Au films. The inset shows TEM image of an individual Ge NW grown by Au catalyst at the tip region. The scale bar is 100 nm for all figures, unless specified otherwise. [(c)–(e)] and [(h)–(j)] are adapted from Ref. 10.

and the stem are single-crystalline, as in the inset of Fig. 1(e), and are respectively indexed to orthorhombic Cu_3Ge and cubic Ge. This observation strongly suggests that Ge NWs precipitate out of Cu_3Ge catalytic tips and is consistent with the phase diagram, as in Fig. 1(b). Often the shapes of the Cu_3Ge tips are not always hemispheric, as typically observed from Au-catalytically grown Ge NWs, with rather irregular interfaces with Ge NWs. It was reported that during the NW growth the solid catalysts (Pd_xSi)-NW (Si) interfaces advances via the lateral propagation of ledges and results in faceted interfaces of several atomic step heights,⁵ and indeed a similar behavior has been observed in the growth of Cu-catalyzed Ge NWs.¹⁶ The observations that Ge NW growth is possible even at 200 °C and that the crystal structures of the catalyst tip are reproducibly identified as Cu_3Ge strongly suggest that the Ge crystals precipitates out from solid Cu_3Ge catalysts, as further follows. According to Fig. 1(b) between 200 and 330 °C, the Ge–Cu systems involve an intermediate phase of solid-solution ϵ_1 (Cu_3Ge) where the Cu content varies around the mean content of 75% by (–)0.1–(+1.9%. One can then speculate that the Ge precipitates out from the supersaturated Cu_3Ge with Cu by up to 1.9% to form Ge NWs, provided that an efficient diffusion across the catalysts is established during the reactions. Under the assumption of the diffusion limited crystallization of Ge NWs, we estimate the lower limit of the Ge diffusivity (D_{Ge}), in order to uphold the NW growth, from the relation, $k_m (=D/r) \geq \nu$, where k_m is the Ge mass transfer rate, ν is the axial growth rate of Ge NWs ($\nu=130$ nm/s in this study), and r is the NW diameter. Then the lower limit of D_{Ge} is found to be 1.08×10^{-13} cm^2/s for the thinnest NW of 5 nm. We find that the bulk diffusivity of Ge in Cu at 275 °C (8.2×10^{-11} cm^2/s) is much greater than its estimated lower limit, thus we suggest that Ge diffusion be possibly available across the Cu_3Ge catalysts for the NW growth. A qualitatively similar growth of Si NWs was reported using Al catalysts at the temperature as low as 430 °C, where the Si solubility in Al is approximately less than 1%.⁶ Therein the solubility of Si in Al is negligible below 400 °C, and this limited solubility presumably imposes the lower limit of the growth temperature. In the Ge–Cu system, however, the Ge solubility in Cu_3Ge is persistently present down to 200 °C from the eutectic temperature, and thus Ge NW growth from the solid Cu_3Ge catalysts can be achievable at such low temperatures. This finding raises an interesting point that upon the existence of thermodynamically available solid-catalysts the appropriate solubility of semiconductors in such solid-catalysts can be an important indicator to determine the lower limit of the attainable growth temperatures. The parallel comparison of Fig. 1 clearly illustrates and contrasts how the Ge NW growth evolves from two different types of catalysts. The Au catalysts were initially scattered as individual nanosized grains, as in Fig. 1(h), and then coalesced into larger grains with embryonic NWs in the very early stage of 5 s growth shown in Fig. 1(i), which suggest that the catalysts are in liquid phases. In the later stage of 30 s growth, as in Fig. 1(j), the diameters of the constituent NWs diverge in their distribution. Meanwhile the Cu catalysts remain as individual grains with the mean diameter of 7.1 nm without

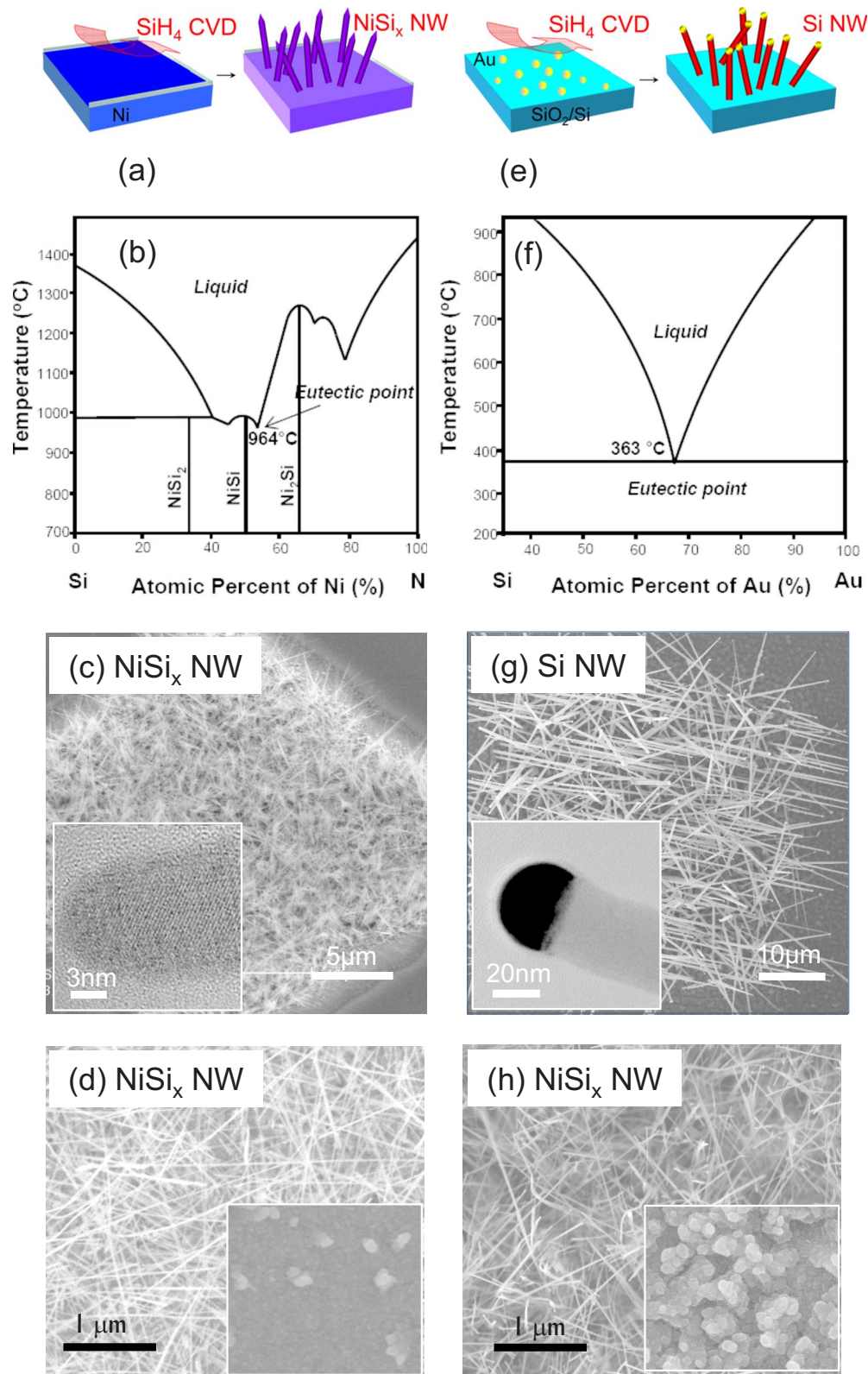


FIG. 2. (Color online) (a) The schematics of the spontaneous NiSi_x NW growth on continuous Ni bulks. (b) A part of the equilibrium Ni-Si binary alloy phase diagram. (c) NiSi_x NWs grown on patterned Ni films. The scale bar is $5\ \mu\text{m}$. The inset shows TEM image of an individual NiSi_x NW at the tip region. (d) A plan-view SEM image of NiSi_x NWs grown at the vapor pressure of 50 Torr of SiH_4 . The inset is the reaction products grown at 200 Torr of SiH_4 . The scale bar is $1\ \mu\text{m}$. (e) The schematics of Si NW growth using SiH_4 vapor precursor at 400°C with discretely distributed Au nanoclusters. (f) A part of the equilibrium Au-Si binary alloy phase diagram. (g) Si NWs grown by the catalytic Au nanoclusters. The scale bar is $10\ \mu\text{m}$. The inset shows TEM image of an individual Si NW at the tip region. (h) A plan-view SEM image of NiSi_x NWs grown on the oxidized Ni films ($\text{NiO} \sim 20\text{nm}$) at the vapor pressure of 50 Torr of SiH_4 . The inset is the reaction products grown on bare Ni surfaces under the same conditions of the main panel. The scale bar is $1\ \mu\text{m}$. (c), (d) and (h) are adapted from Refs. 11 and 12.

any obvious grain growth at the growth temperature, and lead to the growth with the uniform diameters, as consecutively seen in Figs. 1(c)–1(e). That is, we find the diameters of Ge NWs are directly templated from those of Cu catalysts with the one-to-one deterministic manner in their diameters. Whereas in the case of Au-catalytic Ge NWs, the diameter of Ge NWs is ranged in a rather wider distribution, displaying the mean NW diameter of 20 nm from the mean catalyst diameter of 6.5 nm. The uniform diameter distribution of Ge NWs directly templated from that of Cu-catalysts can be another signature that the Cu₃Ge catalysts are in solid-phases and possibly the detrimental coalescence of catalysts¹⁷ that is often observed with liquid-catalysts, can be suppressed during the growth reactions.

III. SPONTANEOUS GROWTH OF NISI NWS FROM BULK NI SEEDS

Figure 2 illustrates the parallel comparison of the schematics and the representative images of the NW products from SiH₄ CVD using Ni and Au catalysts at 400 °C. Figures 2(e)–2(g) represent a typical Au-catalytic Si NW growth, as similarly discussed in the preceding section as a eutectic system. Meanwhile Ni catalysts were prepared by 80 nm thick Ni films on SiO₂/Si substrates, i.e., the Ni catalysts are in continuous bulk films rather than in nanoclusters, as schematically described in Fig. 2(a). Then the prepared Ni films are subsequently loaded into a quartz-tube furnace, where we carry out CVD of SiH₄ at 400 °C. This synthetic approach exploits Ni-catalyzed decomposition of SiH₄,¹⁸ which can occur well below the thermal decomposition temperature of SiH₄ at above 600 °C and usually leads to NiSi_x thin films by silicidations between SiH₄ (g) and Ni(s)—see also Fig. 2(b). Interestingly, however, under the optimum growth conditions, the reaction reproducibly finds the spontaneous growth of NiSi_x NWs in high density on the NiSi_x planar sheets, as seen in Fig. 2(c). Extensive TEM investigations demonstrate that the NWs are single-crystalline NiSi_x with the absence of the catalytic tips, as shown in the inset of Fig. 2(c). Instead we found that the acute-angled tips at the end of the NWs without the presence of any catalyst tip that is the typical characteristics of the Au-catalytic NW syntheses—see also the inset of Fig. 2(g) for comparison. The average diameters of the synthesized NWs are typically ranged from 10 to 15 nm in diameter with a relatively narrow distribution. The spontaneous growth of NiSi_x NWs on continuous Ni bulks without employing nanocluster catalysts can be understood around the roles of Ni seeds as the “self-regulating” one-dimensional nucleation and the subsequent diffusion into NW products. A similar spontaneous NW growth behavior has been documented for vapor-phase syntheses of various silicide NWs, where the metal and/or Si precursors were supplied in vapor-phase.^{19–25} Generally, in vapor-phase syntheses, the relative low supersaturation degree in the vapor-phase favors one-dimensional morphologies due to the limited nucleation, whereas the relatively higher supersaturation leads to the bulk morphology due to the homogeneous nucleation.³ In fact the archetypical examples of such one-dimensional growth in as early as 1953

has been understood within the frame of the nucleation kinetics, where the metal whiskers of various kinds were spontaneously grown by condensation of metal vapors at the low vapor pressures.²⁶ In our example of silicidations between SiH₄ (g) and Ni (s), the spontaneous NiSi_x NW formation, as opposed to the NiSi_x film formation, is determined by the limited supply of not only SiH₄ (g) but also Ni (s) to the reaction surfaces, where Si is supplied by the catalyzed decomposition of SiH₄ (g) and Ni is supplied by the solid-phase diffusion from underlying Ni films. For example, in the Fig. 2(d), the NW formation is facilitated under the relatively low vapor pressure at 50 Torr of SiH₄ (g). At the higher vapor pressure at 200 Torr, the reaction only produces planar NiSi_x sheets, as seen in the inset of Fig. 2(d). The similar trends are observed when Ni surfaces are slightly oxidized to suppress the Ni diffusion flux to the surface reaction with SiH₄ (g), the NiSi_x NWs are spontaneously grown, as in Fig. 2(h). On the bare Ni surfaces, thus at the higher Ni diffusion flux, the reaction products were planar NiSi_x sheets, as seen in the inset of Fig. 2(h). It appears that the limited nucleation kinetics for the spontaneous one-dimensional growth in the *vapor-solid* reactions is closely related to the degree of supersaturation of both solid and vapor phases. Nevertheless the microscopic origins of this self-organized NW growth at the individual NW level is still far from full understanding and requires further investigation

ACKNOWLEDGMENTS

This work was supported by Nano R&D program through the KOSEF (Grant No. 2007-02864), “System IC 2010” project of the MEST, the SRC/ERC program of MOST/KOSEF (Project No. R11-2008-105-01003-0), the KRF Grant MOEHRD (Grant No. KRF-2005-005-J13103), and WCU Program by the MEST (Project No. R31-2008-000-10059-0).

¹R. S. Wagner and W. C. Ellis, *Appl. Phys. Lett.* **4**, 89 (1964).

²A. M. Morales and C. L. Lieber, *Science* **279**, 208 (1998).

³Y. Xia, P. Yang, Y. Sun, Y. Wu, B. Mayers, B. Gates, Y. Yin, F. Kim, and H. Yan *Adv. Mater. (Weinheim, Ger.)* **15**, 353 (2003); C. M. Lieber, and Z. L. Wang, *MRS Bull.* **32**, 99 (2007).

⁴S. Kodambaka, J. Tersoff, M. C. Reuter, and F. M. Ross, *Science* **316**, 729 (2007).

⁵S. Hofmann, R. Sharma, Ch. Wirth, F. Cervantes-Sod, C. Ducati, T. Kasama, R. E. Dunin-Borokowski, J. Druckers, P. Bennett, and J. Robertson, *Nature Mater.* **7**, 372 (2008).

⁶Y. Wang, V. Schmidt, S. Senz, and U. Gösele, *Nat. Nanotechnol.* **1**, 186 (2006).

⁷T. I. Kamins, S. R. Williams, D. P. Basile, T. Hesjedal, and J. S. Harris, *J. Appl. Phys.* **89**, 1008 (2001).

⁸H.-Y. Tuan, D. C. Lee, T. Hanrath, and B. A. Korgel, *Chem. Mater.* **17**, 5705 (2005).

⁹J. L. Lensch-Falk, E. R. Hemesath, F. J. Lopez, and L. J. Laugon, *J. Am. Chem. Soc.* **129**, 10670 (2007).

¹⁰K. Kang, D. A. Kim, H.-S. Lee, C.-J. Kim, J.-E. Yang, and M.-H. Jo, *Adv. Mater. (Weinheim, Ger.)* **20**, 4684 (2008).

¹¹C.-J. Kim, K. Kang, Y. S. Woo, K.-G. Ryu, H. Moon, J.-M. Kim, D.-S. Zang, and M.-H. Jo, *Adv. Mater. (Weinheim, Ger.)* **19**, 3637 (2007).

¹²K. Kang, S.-K. Kim, C.-J. Kim, and M.-H. Jo, *Nano Lett.* **8**, 431 (2008).

¹³B. Massalski, H. Okamoto, P. R. Subramanian, and L. Kacprzak, *Binary Alloy Phase Diagram*, 2nd ed. (ASM International, Materials Park, OH, 1990), Vol. 1.

¹⁴C.-B. Jin, J.-E. Yang, and M.-H. Jo, *Appl. Phys. Lett.* **88**, 193105 (2006).

¹⁵J.-E. Yang, C.-B. Jin, C.-J. Kim, and M.-H. Jo, *Nano Lett.* **6**, 2679 (2006).

- ¹⁶F. M. Ross, personal communication (2008).
- ¹⁷J. B. Hannon, S. Kodambaka, F. M. Ross, and R. M. Tromp, *Nature (London)* **440**, 69 (2006).
- ¹⁸L. H. Dubois and R. G. Nuzzo, *J. Vac. Sci. Technol. A* **2**, 441 (1984).
- ¹⁹C. A. Decker, R. Solanki, J. L. Freeouf, J. R. Carruthers, and D. R. Evans, *Appl. Phys. Lett.* **84**, 1389 (2004).
- ²⁰J. Kim and W. A. Anderson, *Nano Lett.* **6**, 1356 (2006).
- ²¹Y.-L. Chueh, M.-T. Ko, L.-J. Chou, L.-J. Chen, C.-S. Wu, and C.-D. Chen, *Nano Lett.* **6**, 1637 (2006).
- ²²L. Ouyang, E. S. Thrall, M. M. Deshmukh, and H. Park, *Adv. Mater. (Weinheim, Ger.)* **18**, 1437 (2006).
- ²³A. L. Schmitt, M. J. Bierman, D. Schmeisser, F. J. Himpsel, and S. Jin, *Nano Lett.* **6**, 1617 (2006).
- ²⁴Y. Song, A. L. Schmitt, and S. Jin, *Nano Lett.* **7**, 965 (2007).
- ²⁵K. Seo, K. S. K. Varadwaj, P. Mohanty, S. Lee, Y. Jo, M.-H. Jung, J. Kim, and B. Kim, *Nano Lett.* **7**, 1240 (2007).
- ²⁶G. W. Sears, *Acta Metall.* **3**, 367 (1955).